Comparison of Single-Cell Testing, Short-Stack Testing and Mathematical Modeling Methods for a Direct Methanol Fuel Cell

Mustafa Umut Karaoglan,[a,b,*] Alper Can Ince,[c] Andreas Glüsen,[d] C. Ozgur Colpan,[a] Martin Müller,[d] Detlef Stolten[d,e] and Nusret Sefa Kuralay[a]

[a] Dokuz Eylul University, Faculty of Engineering, Mechanical Engineering Department, Tinaztepe, Buca, Izmir, 35397, Turkey
[b] Dokuz Eylul University, The Graduate School of Natural and Applied Sciences, Mechanical Engineering Department, Tinaztepe, Buca, Izmir, 35397, Turkey
[c] Gebze Technical University, Faculty of Engineering, Mechanical Engineering Department, Gebze, Kocaeli, 41400, Turkey
[d] Forschungszentrum Jülich GmbH, Institute of Energy and Climate Research - Electrochemical Process Engineering (IEK-3), 52425, Jülich, Germany
[e] Chair for Fuel Cells, RWTH Aachen University, C/o Institute of Electrochemical Process Engineering (IEK-3), Forschungszentrum Jülich GmbH, Wilhelm–Johnen–Str., D52428, Germany
* E-mail: mustafa.karaoglan@deu.edu.tr

Abstract

In this paper, a comparison between direct methanol fuel cell (DMFC) measurements performed on a single cell and a short-stack, and the results of a mathematical model for a DMFC, is presented. The testing of a short-stack, which consists of 5 cells with an active area of 315 cm^2, was performed at various current densities, permeation current densities, and cathode flow rates (CFR) in order to determine the voltage outputs of each cell. Methanol concentration and stack temperature results obtained from short-stack testing were then integrated into the single cell test and single cell mathematical model as the input parameters. For the mathematical modelling, transport equations originating from methanol, water, and oxygen were coupled with the electrochemical relations. Therefore, a comparison between these three methods is made in order to gain a deeper understanding of the effects of the operating parameters on DMFC performance. This study showed that the model could describe experimental results well when lower methanol concentrations (under 1.2 M) and temperature (under 60 °C) values are used as input parameters. The results also show very good agreement at lower methanol permeation rates and therefore lower temperatures. It is found that the voltage output for a given current density is higher for the theoretical model than that of the experimental studies; and the differences in the results can be up to 0.04 V for a cell.

Keywords: Direct methanol fuel cell, Short-stack test, Single cell test, Single cell model, 1D-model

1. Introduction

The growing demand to obtain clean energy has made fuel cell (FC) technology more attractive in recent decades. This technology not only has lower environmental impacts but also features higher energy conversion efficiency and quieter operation. However, the high cost of FC materials has been a challenge for its commercialization in the market. Solid oxide fuel cells (SOFCs) and proton exchange membrane fuel cells (PEMFCs) lead in stationary applications (e.g., power generation, cogeneration or trigeneration) and vehicle applications, respectively. On the other hand, direct methanol fuel cells (DMFCs) are considered promising candidates for portable power applications. The DMFC offers a compact design, as it does not require a fuel reformer, operates at comparatively low temperatures compared to some types of FCs (e.g., SOFCs), and methanol, which has a high energy density, can be simply stored in liquid form in a tank [1-3]. Therefore, DMFCs can be a good option for producing power in mobile homes, boats, and forklifts as a secondary power source [4-6]. However, high methanol permeation and lower reaction kinetic rates are issues that must be addressed in order to achieve better performance.

As the main performance criterion, voltage output depends on many parameters, such as current density, methanol concentration, operating temperature, anode volume flow rates (AFR), and cathode volume flow rates (CFR) in DMFCs. Comprehensive studies have been carried out, both experimentally [3, 7, 8] and theoretically [6, 9], to determine the best operating conditions for performance in DMFCs.

For example, Wang et al. [9] conducted study on cell performance (e.g. anode/cathode activation losses, ohmic loses in electrolyte and mass transfer losses in gas diffusion layer) under variable methanol concentrations (0.5 M, 1 M and 2 M) and operating temperature (45 °C, 60 °C and 75 °C) experimentally. They reported that the total overpotentials could be decreased by adjusting operating conditions. However, they found that the proportion of activation loss in total loss does not show significant change by adjusting operating conditions. The cell performance of a DMFC was investigated by Jung et al. [10] for various membrane types (Nafion 117, 115 and 112) and operating temperatures from 60 °C to 120 °C. They obtained the highest power density at 0.55 V and 0.23 $A \cdot cm^{-2}$ by using a 2.5 M methanol concentration and Nafion 112 membrane. A single cell test was performed by Ge et al. [11] for different methanol concentrations (from 0.5 M to 6 M), cathode humidification temperatures (CHT, from 40 °C to 90 °C), and methanol flow rates (from 0.5 ml/min to 10 ml/min); the results showed that the effect of CHT on cell performance was not significant. However, when the CHT is increased up to a higher temperature, such as 90 °C, the amount of water produced, mostly liquid, by electro-osmosis and permeation mechanisms is decreased, even though the cell performance does not change. In addition, the optimum methanol concentration was found to be between 1-2 M. Thomas et al. [12] conducted a study to assess the cathode performance of a DMFC with the change of air temperature and cathode Pt loading. This study showed that sufficient Pt loading of the cathode enables to lower cathode polarization of 20 mV at 0.10 $A \cdot cm^{-2}$ when the DMFC working conditions are optimized. In addition, a semi-empirical model for a single cell was developed by Dohle et al. [13] using the results of an experimental study of a DMFC for various methanol concentrations (0.25 M-2 M) and operating temperatures (30-70 °C); the results indicated that a higher power output was obtained when the methanol concentration was 0.25 M in a low current densities regime (<0.10 $A \cdot cm^{-2}$) and the methanol concentration was 0.5 M in high current densities (>0.10 $A \cdot cm^{-2}$).

On the other hand, the development of a DMFC stack and determination of its operational characteristics were studied for many different size and power outputs. Short DMFC stacks were developed for 33 W [14], 40 W [15] and 50 W [16] power outputs and their performances were presented for various CFR, stack temperature and methanol concentrations. Evaluation of large-scale DMFC stack operation was also presented in the literature surveys. For example, Joh et al. [17] performed an experimental study on a 42-cell DMFC (400 W) stack with an active area of 138 cm^2 to investigate the temperature in each cell unit for different methanol concentrations and pressure drops on the anode and cathode sides for variable AFRs, as well as methanol concentrations. The results showed that uniform temperature distribution amongst the cells was obtained at 0.8 M and 0.5 M methanol concentrations. A lower methanol concentration leads to an increased pressure drop on the anode side with increasing AFR. In addition, the long term operation of a stack was carried out and slight degradation was observed during the first 500 h. Schulze Lohoff et al. [18] conducted a study on DMFC short stack characterization, which includes voltage, methanol permeation and water permeation, using design of experiment methodology from their experimental data. For this purpose, three inputs (temperature, methanol concentration and current density) were determined using quadratic regression model; and model coefficients were predicted. Finally, through this principle, they obtained the minimized 15 measurement points to predict methanol permeation, voltage, and water permeation. Dohle et al. [19] experimentally tested the viability of the operating conditions of a DMFC at the cell, short stack and long stack levels. The power density obtained from a heated single cell and long stack of a DMFC without heating showed similarity and was higher than the power density of the short stack without heating at the current density and methanol concentration of 0.20 $A \cdot cm^{-2}$ and 1 M, respectively. At this point, the operating temperature of a single cell was 77 °C, while the temperatures of the short stack and long stacks were 45 and 64 °C, respectively. Single cells and long stacks of a DMFC can be operated with high current densities at these temperatures, unlike short stacks.

In addition to the experimental studies, single-cell mathematical models of DMFCs were investigated to predict the results more quickly and economically and to understand the reasons behind the trends in the results better. For 0D to 3D, modeling studies for DMFCs were conducted in the literature. For example, methanol crossover rate was calculated by Garcia et al. [20] through a 1D DMFC mathematical model. A semi-empirical and 1D DMFC model was developed by Oliveira et al. [21], and they compared the results with those from analytical calculations for different methanol concentrations (from 0.25 to 2 M) and operating temperatures (85 °C and 110 °C). Moreover, a 1D DMFC stack model was developed by Lee et al. [22] to integrate the stack model into the system-level model. Hence, the effect of short stack performance on the DMFC system performance was investigated at different operating conditions. In another study, a 1D model of a flowing electrolyte DMFC was developed by Colpan et al. [6] to create the polarization curve, power density and methanol concentration distribution for various methanol concentrations. Colpan et al. [23] developed a 2D model for a flowing electrolyte DMFC and showed the

methanol and oxygen concentration distributions in fuel and air channels in the flow and thickness directions. Furthermore, more comprehensive investigations were performed using a 3D modeling approach to assess the effects of the operating conditions on DMFC performance [24-26].

While some efforts could be placed on comparisons between the test and numerical results for both single cell and stack studies, only a few reports are related to DMFCs. Casalegno et al. [27, 28] presented the validation of a model for a single-cell DMFC through experimental analysis. In another study, experimental and numerical studies of a micro-DMFC were implemented by Falcao et al. [29] using a 1D cell model to compare the voltage outputs, methanol crossover for different methanol concentrations and the air and methanol flow rates.

Unlike the studies found in the literature, in this study, a comparison which includes mathematical modeling for a single cell, single-cell testing and short-stack testing of a DMFC is presented to determine cell performance. Cell performance at various cathode air flow rates, temperatures, methanol concentrations and methanol crossover current densities is then compared. As a result, the strengths and weaknesses of each of these three methods are shown for DMFC characterization. In each level of DMFC characterization, certain effects can be controlled especially well, while other effects cannot be. Therefore, it is useful to compare different methods in order to gain a deeper understanding of the effects of the operating parameters on DMFC performance.

2. Method

2.1. Short stack testing

At the Forschungszentrum Jülich in Germany, performance testing of a short stack consisting of 5 cells is conducted with the DMFC short stack test rig shown in Figure 1. The test rig control uses current density, methanol permeation and air flow rate as input parameters. Temperature and methanol concentration are obtained as output parameters. The input methanol crossover current density is initially not the real methanol crossover. If the real crossover is, for example, higher, more methanol is consumed in the stack than is added by the methanol pump, and so the methanol concentration and therefore also methanol crossover will decrease until an equilibrium is reached and the real crossover is equal to the input crossover current density. Temperature control is performed by controlling the thermostat, so that the methanol solution entering the stack has the same temperature as that leaving it. Thus, the thermal losses of the mixing vessel and tubes are compensated for. The thermal losses of the stack are reduced by insulation, but small losses must still be taken into account. It can be assumed that the first and last cells lose some heat over the end plates and are therefore a little cooler than the cells in the middle. The temperature of the stack is mainly defined by electrochemical losses (methanol permeation and the cell voltage being lower than the voltage defined by the lower heating value of methanol), heating the stack and the evaporation of water at the cathode cooling the stack until an equilibrium is reached.

Experiments were performed at various current densities (i), methanol crossover current density (i_{Perm}) and CFR (V_C). According to the methanol permeation input in the experiment, the methanol concentration can be measured as a function of methanol permeation. This also means that the concentrated methanol is refilled into the anode mixing vessel according to the current density and the methanol permeation. After a few hours (generally 1-3), a constant concentration is established and can be measured. The operating principles of the test rig shown in Figure 1 can be explained as follows: A methanol-water solution is fed into the anode side of the DMFC from a mixing vessel. Methanol is pumped into the mixing vessel and its flow rate is controlled by a methanol pump. The short stack testing system is controlled by a computer to control the test parameters. A load unit consumes the current generated in the stack, a data logger reads the voltage response of the DMFC, a mass flow controller controls the air flow to the cathode, a refractometer measures the methanol concentration and a thermostat heats the methanol solution to the temperature of the methanol outlet to compensate for heat loss in the anode mixing vessel and tubes. In addition, temperatures are measured by thermometers at the anode inlet, anode outlet and cathode outlet.

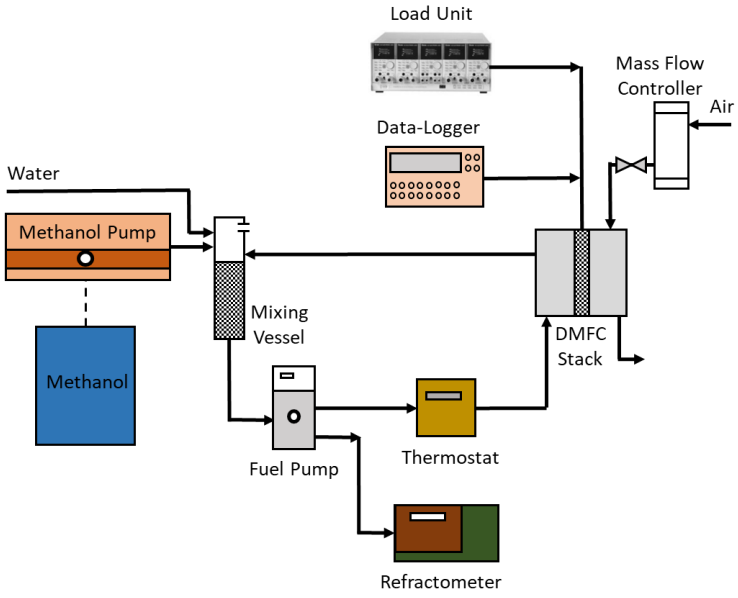

Figure 1. DMFC short stack test rig.

The DMFC short stack consists of five cells with a 315 cm^2 active area that have Johnson Matthey membrane electrode assemblies (MEA0630). External stack-dimensions are 27*21 cm^2 cell area, including sealing area, bolts and manifolds. The stack thickness is 7.4 cm, including 1.7 cm for the 5 cells (cell pitch is 3.4 mm) and 5.7 cm for the end plates. This design has been used with up to 120 cells in a stack with 2kW nominal power output [30]. However, 5 cells are sufficient to study the interactions of operating parameters under self-heating conditions. Depending on the operating conditions, a nominal power density of 0.050-0.075 mW/cm² can be assumed over the lifetime of the stack, while the maximum power density at the beginning of life is approximately 0.1 W/cm². Thus the 5-cell stack has a power output of 78.75 to 157.5W.

To measure the performance of the DMFC short stack under various conditions, the input parameters for short stack testing are shown in Table 1. In the first step of the test procedure, the stack was heated up by heating the anode inlet to 70 °C for 1 h (anode inlet temperature symbolized with T_A) at a 0.22 $ml \cdot cm^{-2} \cdot min^{-1}$ anode flow rate (V_A), 10 $ml \cdot cm^{-2} \cdot min^{-1}$ cathode flow rate (V_C), 0.075 $A \cdot cm^{-2}$ crossover current density (i_{Perm}) and zero current density. Then, the experiments were performed with three current densities (i) at 0.10, 0.15 and 0.20 $A \cdot cm^{-2}$ and three crossover current densities (i_{Perm}) at 0.05, 0.01 and 0.15 $A \cdot cm^{-2}$ individually for various cathode flow rates changed between 10 and 30 $ml \cdot cm^{-2} \cdot min^{-1}$. Each operating step was maintained for 3 hours to reach equilibrium. In order to cancel the reversible degradation, operation was interrupted for 28 seconds after 1800 s of operation [31]. The interruption consists of three phases for 3, 15 and 10 s with cathode flow rate inputs (V_{Ci}) of the previously set values of 0 and 35 $ml \cdot cm^{-2} \cdot min^{-1}$, respectively. At the end of testing, there is a 2 h (7200 s) cooling down step to a 35 °C operating temperature with a 0.22 $ml \cdot cm^{-2} \cdot min^{-1}$ anode flow rate (V_A) and 10 $ml \cdot cm^{-2} \cdot min^{-1}$ cathode flow rate (V_C), 0.075 $A \cdot cm^{-2}$ methanol crossover current density (i_{Perm}) and zero current density. The resulting temperatures and concentrations of the short stack testing are shown in Table 2 and are used as input parameters for single cell testing.

Table 1. Input parameters of the short stack test; n/a means that the parameter is a measured output parameter in this operating phase.

Purpose	Number of repetitions	t [s]	i [$A \cdot cm^{-2}$]	V_A [$ml \cdot cm^{-2} \cdot min^{-1}$]	V_C [$ml \cdot cm^{-2} \cdot min^{-1}$]	i_{Perm} [$A \cdot cm^{-2}$]	T_A [°C]	ΔT [°C]
Heating	1	3600	0	0.22	10	0.075	70	n/a
for each V_{Ci} of 10-12-15-20-25-30	6	1800	0.10	0.30	V_{Ci}	0.050	n/a	0
		3	0	0.30	V_{Ci}	0.050	n/a	0
		15	0	0.30	0	0.050	n/a	0
		10	0	0.30	35	0.050	n/a	0
for each V_{Ci} of 10-12-15-20-25-30	6	1800	0.15	0.30	V_{Ci}	0.050	n/a	0
		3	0	0.30	V_{Ci}	0.050	n/a	0
		15	0	0.30	0	0.050	n/a	0
		10	0	0.30	35	0.050	n/a	0

		1800	0.20	0.30	V_{Ci}	0.050	n/a	0
for each V_{Ci} of 10-12-15-20-25-30	6	3	0	0.30	V_{Ci}	0.050	n/a	0
		15	0	0.30	0	0.050	n/a	0
		10	0	0.30	35	0.050	n/a	0
		1800	0.10	0.30	V_{Ci}	0.100	n/a	0
for each V_{Ci} of 10-12-15-20-25-30	6	3	0	0.30	V_{Ci}	0.100	n/a	0
		15	0	0.30	0	0.100	n/a	0
		10	0	0.30	35	0.100	n/a	0
		1800	0.15	0.30	V_{Ci}	0.100	n/a	0
for each V_{Ci} of 10-12-15-20-25-30	6	3	0	0.30	V_{Ci}	0.100	n/a	0
		15	0	0.30	0	0.100	n/a	0
		10	0	0.30	35	0.100	n/a	0
		1800	0.20	0.30	V_{Ci}	0.100	n/a	0
for each V_{Ci} of 10-12-15-20-25-30	6	3	0	0.30	V_{Ci}	0.100	n/a	0
		15	0	0.30	0	0.100	n/a	0
		10	0	0.30	35	0.100	n/a	0
		1800	0.10	0.30	V_{Ci}	0.150	n/a	0
for each V_{Ci} of 10-12-15-20-25-30	6	3	0	0.30	V_{Ci}	0.150	n/a	0
		15	0	0.30	0	0.150	n/a	0
		10	0	0.30	35	0.150	n/a	0
		1800	0.15	0.30	V_{Ci}	0.150	n/a	0
for each V_{Ci} of 10-12-15-20-25-30	6	3	0	0.30	V_{Ci}	0.150	n/a	0
		15	0	0.30	0	0.150	n/a	0
		10	0	0.30	35	0.150	n/a	0
		1800	0.20	0.30	V_{Ci}	0.150	n/a	0
for each V_{Ci} of 10-12-15-20-25-30	6	3	0	0.30	V_{Ci}	0.150	n/a	0
		15	0	0.30	0	0.150	n/a	0
		10	0	0.30	35	0.150	n/a	0
Cooling	1	7200	0	0.22	10	0.075	35	n/a

2.2. Single cell testing

Single cell testing of the DMFC is performed in a cell test rig for various current density (i), operating temperature (T_A), CFR (V_C) and methanol concentration (C_{MeOH}) values. In contrast to the short stack test rig, the cell temperature is an input parameter and the cell temperature is maintained with heating. Thus, it is possible to study the operating conditions, which could not be achieved with a self-heating stack. These unrealistic operating conditions were avoided by using the operating parameters obtained in the self-heating stack test rig (see Table 2).

Table 2. Results of short stack testing and the input parameters of the single cell test.

No	**i** [A·cm^{-2}]	**V_C** [ml·cm^{-2}·min^{-1}]	**C_{MeOH}** [mole·l^{-1}]	**T_A** [°C]	**No**	**i** [A·cm^{-2}]	**V_C** [ml·cm^{-2}·min^{-1}]	**C_{MeOH}** [mole·l^{-1}]	**T_A** [°C]	**No**	**i** [A·cm^{-2}]	**V_C** [ml·cm^{-2}·min^{-1}]	**C_{MeOH}** [mole·l^{-1}]	**T_A** [°C]
1	0.10	10	1	76	***16***	0.15	15	0.95	67	***31***	0.15	20	1.4	59
2	0.15	10	1	76	***17***	0.15	12	0.55	66	***32***	0.15	20	0.7	59
3	0.20	15	1.1	74	***18***	0.10	15	1	65	***33***	0.10	15	0.65	58
4	0.15	12	1.1	74	***19***	0.10	10	0.55	65	***34***	0.20	30	1.4	58
5	0.10	10	1.1	73	***20***	0.20	25	1	64	***35***	0.15	30	1.1	57
6	0.10	10	0.8	73	***21***	0.15	20	1	63	***36***	0.15	25	1.5	57
7	0.15	15	1.2	71	***22***	0.15	20	0.7	63	***37***	0.20	30	0.75	57
8	0.10	12	0.5	71	***23***	0.20	20	1.2	63	***38***	0.10	25	1.1	56
9	0.10	15	0.9	70	***24***	0.15	15	0.6	63	***39***	0.15	25	0.75	55
10	0.15	12	0.9	70	***25***	0.10	12	0.6	62	***40***	0.10	20	1.5	55
11	0.10	10	0.9	70	***26***	0.20	30	0.95	61	***41***	0.15	30	1.5	54
12	0.15	10	0.5	69	***27***	0.10	25	1.3	60	***42***	0.10	30	1.1	53
13	0.10	12	0.95	68	***28***	0.15	25	1	60	***43***	0.15	25	1.5	53
14	0.20	20	1	68	***29***	0.20	25	0.75	60	***44***	0.10	20	0.75	53
15	0.10	15	1.25	67	***30***	0.10	20	1.1	59	***45***	0.15	30	0.8	52

The layout of the single cell test rig is illustrated in Figure 2. Its operation is explained as follows: Different methanol concentrations are supplied by mixing solutions from a water tank, 0.75 M and 3 M methanol tanks. The single cell test system measures the cell voltage output and permeation current density as a result of these input parameters. A computer controls the operating temperature of the cell and cathode flow rate by means of a mass flow controller (MFC). Data on the results are collected by the voltmeter and transmitted to the computer simultaneously. A DC electronic load unit is used for the arrangement of the required current density of the cell. The single cell test system contains a heating cell to heat the methanol solution before it enters the cell. During the tests, the evaporator is used to heat up the gases leaving the cathode of the DMFC to 130 °C in order to make sure that all water at the cathode outlet is in the vapor phase. In the condenser, the water and non-condensable gases are separated. The water is removed from the system while the non-condensable gases reach the top of the condenser. Here, the CO_2 concentration was measured by a CO_2 sensor. As the CO_2 is generated due to the fact that methanol crossed over to the cathode reacts with oxygen, the molar flow rate of methanol crossover can be obtained from the measured CO_2. The methanol crossover current density can be calculated from the molar flow rate of methanol crossover using Faraday's Law [32].

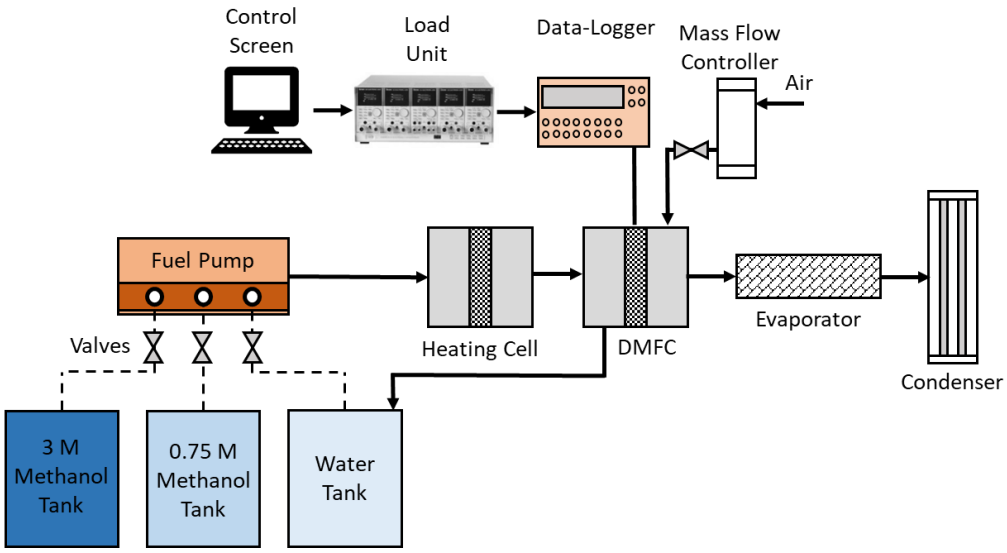

Figure 2. Single cell test system for the DMFC.

An MEA from Johnson Matthey Fuel Cells (MEA 0630) with a 4.2 cm x 4.2 cm active area was sealed on both the anode and cathode sides by means of 0.2 mm PTFE flat gaskets. The anode and cathode flow fields had a checkerboard structure with 1 mm as the width and depth of the channels, as well as the width of the lands. The flow fields were machined from graphite plates. The end plate was made using stainless steel with a size of 12 mm x 90 mm x 90 mm.

Before operating the cell with the investigated input parameters, methanol was fed into the anode after heating up to 76 °C for 2 h with a 0.2 $ml \cdot cm^{-2} \cdot min^{-1}$ anode flow rate. Then, measurements with the required operating parameters for various current densities (i) between 0.01 and 0.25 $A \cdot cm^{-2}$, CFR (V_C) between 10 and 30 $ml \cdot cm^{-2} \cdot min^{-1}$, methanol concentrations (C_{MeOH}) between 0.5 M and 1.5 M, and anode temperatures (T_A) between 76 °C and 52 °C of the DMFC single cell were performed to compare with short stack test results for the same input parameters. Table 3 shows the input parameters for each measurement condition, which were maintained for 2 h.

2.3. 1D modeling of a DMFC

The voltage output of a DMFC for a given current density was calculated using a 1D cell model, as described in the study by Colpan et al. [5]. For this purpose, the transport equations of water, methanol and oxygen were coupled to those originating from electrochemistry. This model gives the voltage losses, cell voltage and power density of a DMFC. It is based on the following main assumptions:

- The cell operates at a constant temperature and pressure and under steady state conditions [6, 24, 25].
- Only the liquid phase is considered on the anode side [6].
- Methanol permeated to the cathode is fully consumed at the cathode catalyst layer [6].
- Contact resistances and the resistance to the electrons are neglected.

A schematic diagram of the mathematical model is illustrated in Fig. 3 based on the input parameters and system equations to find cell voltage theoretically.

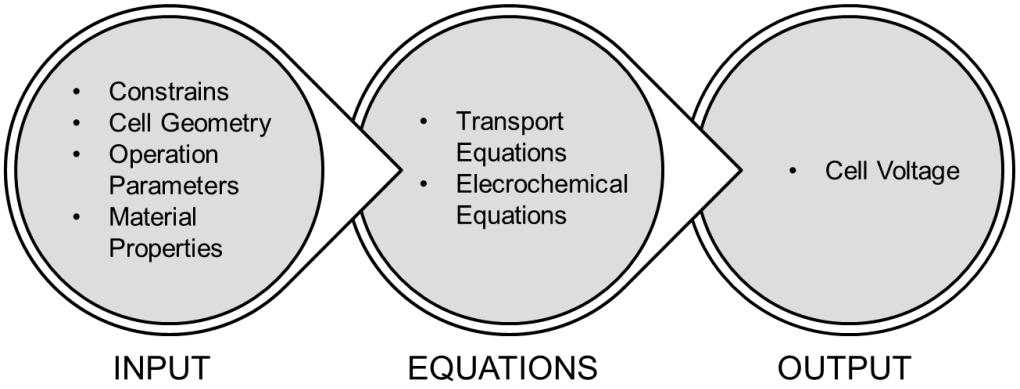

Figure 3. Schematic diagram of the mathematical model

For the 1D DMFC model, the general form of the transport equation for methanol, oxygen and water can be shown as follows:

$$-D\frac{\partial^2 C}{\partial x^2} + u\frac{\partial C}{\partial x} = S \tag{1}$$

where D is the coefficient of diffusion, x is the thickness direction, C is the concentration of species of interests, u is the fluid velocity and S is the source term [6].

Although the Nerst voltage in a DMFC (V_N) is 1.103 V, lower voltage outputs from the cell were achieved due to the activation, ohmic, concentration and methanol crossover losses. The cell voltage can be calculated for a DMFC according to the following equation:

$$V_{cell} = V_N - \eta_{act} - \eta_{ohm} - \eta_{conc} \tag{2}$$

Activation losses can be expressed for both the anode and cathode as follows:

$$\eta_{act}^{a} = \left(\frac{R\cdot T}{\alpha_a \cdot F}\right) \cdot ln\left(\frac{i}{i_{oa}}\right) \tag{3}$$

$$\eta_{act}^{c} = \left(\frac{R\cdot T}{\alpha_c \cdot F}\right) \cdot ln\left(\frac{i+i_{perm}}{i_{oc}}\right) \tag{4}$$

where T is the operating temperature (K), R is the universal gas constant ($J\cdot K^{-1}\cdot mol^{-1}$), F is the Faraday constant ($s\cdot A\cdot mol^{-1}$), i is the current density ($A\cdot cm^{-2}$), i_{oa} and i_{oc} are the exchange current densities for the anode and cathode ($A\cdot cm^{-2}$), α_a and α_c are the transfer coefficients for the anode and cathode and i_{perm} is the methanol crossover current density ($A\cdot cm^{-2}$).

Ohmic loss is caused by resistance to the ions, electrons and contact between the components [5]. It depends on the thickness (t) and conductivity (σ) of the layers of the cell, as shown below:

$$\eta_{ohm} = i \cdot \left(\sum \frac{t}{\sigma}\right) + R_{contact} \tag{5}$$

Concentration losses are expressed for the anode and cathode as follows:

$$\eta_{conc}^{a} = \left(\frac{-R \cdot T}{v_a \cdot F}\right) \cdot ln\left(1 - \frac{i}{i_{lim,a}}\right) \quad (6)$$

$$\eta_{conc}^{c} = \left(\frac{-R \cdot T}{v_c \cdot F}\right) \cdot ln\left(1 - \frac{i}{i_{lim,c}}\right) \quad (7)$$

where v_a and v_c are the numbers of protons produced or consumed per one mol of reactant and $i_{lim,a}$ and $i_{lim,c}$ are the limiting current densities at the anode and cathode, respectively. The formulation of the limiting current densities for anode and cathode ($i_{lima,c}$) is shown in below:

$$i_{lima,c} = \frac{n_{a,c} \cdot F \cdot D_{a,c} \cdot C_{a,c}}{t_{a,c}} \quad (8)$$

where $n_{a,c}$ is taken to be 6 for the anode, 4 for the cathode, as it represent the number of protons produced or consumed per one mol of reactant, $D_{a,c}$ is the coefficient of diffusion for the relevant backing layer, $C_{a,c}$ is the methanol concentration at the anode and oxygen concentration at the cathode and $t_{a,c}$ is the thickness of the anode or cathode catalyst layer. The input parameters of the 1D cell model are presented in Table 3.

Table 3. Main input parameters of the 1D single cell DMFC model.

Input parameters	Value	Unit
Thickness of the anode backing layer	0.014	cm
Thickness of the anode catalyst layer	0.001	cm
Thickness of the membrane	0.0127	cm
Thickness of the cathode catalyst layer	0.004	cm
Thickness of the cathode backing layer	0.014	cm
Porosity of the anode backing layer	0.6	-
Porosity of the cathode backing layer	0.6	-
Pressure of the cathode	101.3	kPa
Anodic transfer coefficient	0.24	-
Cathodic transfer coefficient	0.87	-
Conductivity of the membrane	0.2	$S \cdot cm^{-1}$

3. Results and discussion

The short stack test results for average cell voltage are shown in Figure 4 for the set values for the methanol crossover current density (i_{perm}), which are 0.05 $A \cdot cm^{-2}$, 0.10 $A \cdot cm^{-2}$, and 0.15 $A \cdot cm^{-2}$. The short stack test procedure was arranged for 0.10 $A \cdot cm^{-2}$, 0.15 $A \cdot cm^{-2}$, and 0.20 $A \cdot cm^{-2}$ current densities (i), with their operating zones are marked in Figure 4. In addition, each zone of related current density includes three CFR (v_C) values of 10, 12 and 15 $ml \cdot cm^{-2} \cdot min^{-1}$ (Figure 4a) and 20, 25 and 30 $ml \cdot cm^{-2} \cdot min^{-1}$ (Figure 4b) according to the input parameter of short stack testing, which is detailed in the test procedure table in Section 2.1. According to the characteristics of the data logger at the stack test station, data have been saved every 10 seconds during the test. Therefore, stack performance is plotted for the number of data points which are collected every 10 seconds. In Figure 4a, the average voltage is higher, with 0.05 $A \cdot cm^{-2}$ methanol crossover current density for a 0.10 $A \cdot cm^{-2}$ current density; however, higher cell voltage is achieved at a 0.10 $A \cdot cm^{-2}$ methanol crossover current density for a 0.20 $A \cdot cm^{-2}$ current density and 10 $ml \cdot cm^{-2} \cdot min^{-1}$ CFR. Operation of the short stack was not possible at some operating conditions and no average voltage could be obtained. This is due to the cathodic air flow rate, which was not sufficient for generating a high current density and oxidizing a large amount of permeated methanol at the cathode at the same time. Reliable operation was not achieved at 0.15 $A \cdot cm^{-2}$ i – 10 $ml \cdot cm^{-2} \cdot min^{-1}$ CFR, nor 0.20 $A \cdot cm^{-2}$ i – 10, 12 $ml \cdot cm^{-2} \cdot min^{-1}$ CFR at 0.15 $A \cdot cm^{-2}$ i_{perm}, nor 0.20 $A \cdot cm^{-2}$ i – 10 $ml \cdot cm^{-2} \cdot min^{-1}$ CFR at 0.05 and 0.10 $A \cdot cm^{-2}$ i_{perm}. However, the failure was not observed for the higher CFR average cell voltage of the stack and the results showed more regular characteristics, as can be seen in Figure 3b.

In Figure 4b, higher cell voltages were observed at a 0.10 $A \cdot cm^{-2}$ permeation current density for all current densities, and the average cell voltage increased by about 0.1 V when the CFR changed from the higher value 30 $ml \cdot cm^{-2} \cdot min^{-1}$ to the lower one of 20 $ml \cdot cm^{-2} \cdot min^{-1}$ at each current density. For example, the average cell voltage was 0.36 V for 30 $ml \cdot cm^{-2} \cdot min^{-1}$ CFR, 0.37 V for 25 $ml \cdot cm^{-2} \cdot min^{-1}$ CFR and 0.38 V for 20 $ml \cdot cm^{-2} \cdot min^{-1}$ CFR. Hence, it can be stated that a higher average cell voltage could be achieved from the stack with lower values of CFR under lower current density conditions; but using higher CFR offers reliable operation, despite the lower voltage. Xu et al. [33] also showed that higher air

flow rate could not ensure a reliable cell performance due to the less water content in the membrane at higher CFRs. The less water content in the membrane leads to a decrease in the anode reaction kinetics.

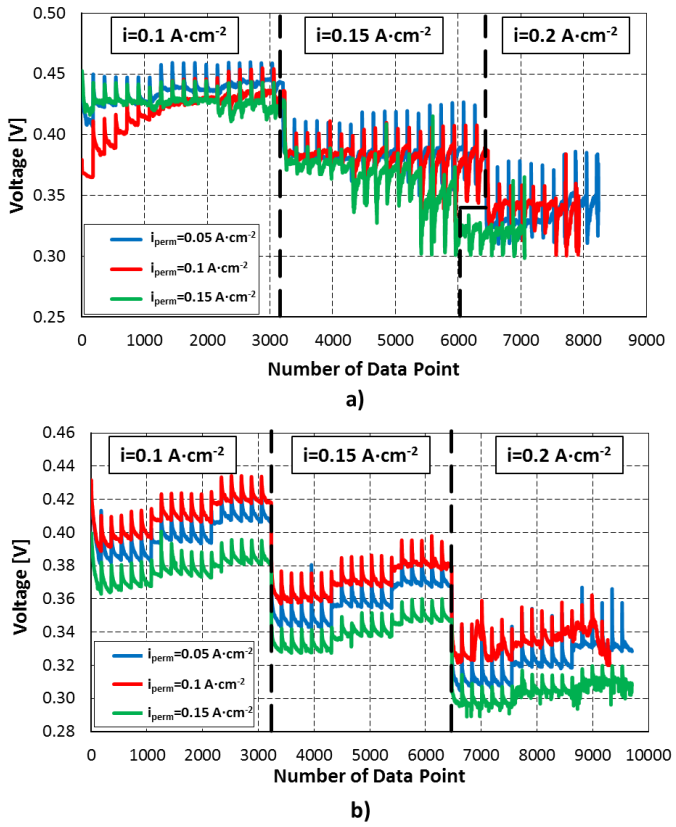

Figure 4. Test results of the average cell voltage from the short stack at 0.1 A·cm^{-2}, 0.15 A·cm^{-2} and 0.2 A·cm^{-2} current density for: (a) lower CFR (10, 12, 15 ml·cm^{-2}·min^{-1}); and (b) higher CFR (20, 25, 30 ml·cm^{-2}·min^{-1}).

Although the single cell test conditions are arranged according to the short stack results for the comparison, the results from the single cell test rig are utilized for three methanol concentrations (0.5 M, 1 M and 1.5 M) and three CFRs (10, 20 and 30 ml·cm^{-2}·min^{-1}) to investigate the performance characteristics of the single cell. The results are shown in the Figure 5 for a 70 °C operating temperature. Although a higher voltage can be observed at lower current densities at 0.5 M methanol concentration, the cell voltage increasingly drops after the 0.15 A·cm^{-2} current density at all values of the CFR. It is shown that the effect of the CFR on cell voltage is almost negligible across the entire current density range. The highest outputs are achieved between 0.55 V and 0.45 V at current densities below 0.15 A·cm^{-2} with 0.5 M concentration, and between 0.45 V and 0.36 V at current densities above 0.15 A·cm^{-2} with 1 M concentration. On the other hand, cell performance decreases at 0.5 M concentration at higher current densities because there is not sufficient methanol in the solution to meet the current demand. It is expected that higher voltages could be obtained for current densities higher than 0.25 A·cm^{-2} with a 1.5 M methanol concentration if higher current densities were investigated in single cell tests. However, the range between 0.05 A·cm^{-2} and 0.25 A·cm^{-2} is considered to be sufficient to make a comparison with the average cell voltage results for the short stack.

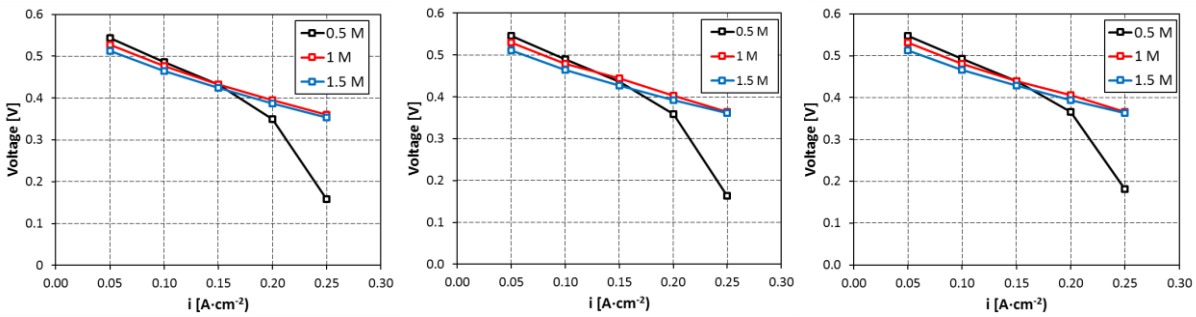

Figure 5. Single cell test results of 0.5 M, 1 M and 1.5 M methanol concentrations for 10 ml·cm^{-2}·min^{-1} CFR (a), 20 ml·cm^{-2}·min^{-1} CFR (b), 30 ml·cm^{-2}·min^{-1} CFR (c) at a 70 °C operating temperature.

In order to compare the results of the DMFC short stack and single cell, the numerical model described in Section 2.3 is used to study the effect of operating temperature and methanol concentration on DMFC performance. The results of 1D cell modelling are presented in Figure 6 for 0.5 M, 1 M and 1.5 M methanol concentrations at the feed stream and the cell temperature was taken as 60 °C and 70 °C. However, flow rates at the cathode and anode inlet were not used as the input parameters because of the limitations of the 1D modeling approach applied in this paper. Although the voltage output of a cell is a bit higher, at 0.5 M under 0.10 A·cm^{-2}, lower cell voltages can be observed at current densities higher than 0.09 A·cm^{-2} and 0.12 A·cm^{-2} at 60 °C and 70 °C, respectively, for 0.5 M. It can clearly be seen that the operating temperature has a larger effect than the methanol concentration on the cell voltage. It is because that the change of temperature has a significant effect on both methanol crossover and electrode activation [3, 34 and 35]. For example, Ercelik et al. [3] reported that an increment of temperature increases the anode and cathode reaction rates. However, it leads to an increase in the methanol crossover.

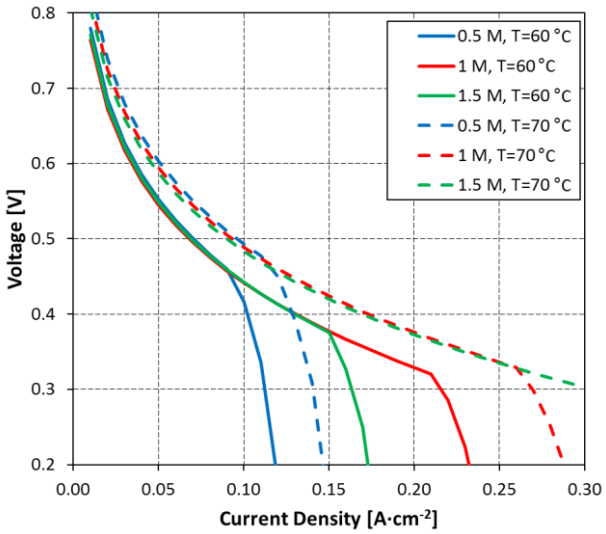

Figure 6. 1D DMFC model polarization results for 0.5 M, 1 M and 1.5 M at 60 °C and 70 °C operating temperatures.

A comparison of the cell voltage calculated numerically and measured by the single cell testing and short stack testing (average cell voltage for this case) is presented in Figure 7. The left sides of Figure 6a-6c show the change of cell voltage with the methanol concentration for the current density values of 0.10 A·cm^{-2}, 0.15 A·cm^{-2} and 0.20 A·cm^{-2}, respectively. In addition, the change in the operating parameters, which are the cell temperature, methanol permeation and cathode flow rate, with methanol concentration, are shown on the right-hand side of these figures. The required operating parameters, which were arranged according to the short stack test results, were defined in Section 2.2 and Table 2 for single cell testing. However, the comparison results, which are presented in Figure 7, do not comprise the results for each set of input parameters because of the failures in single cell testing at lower temperatures.

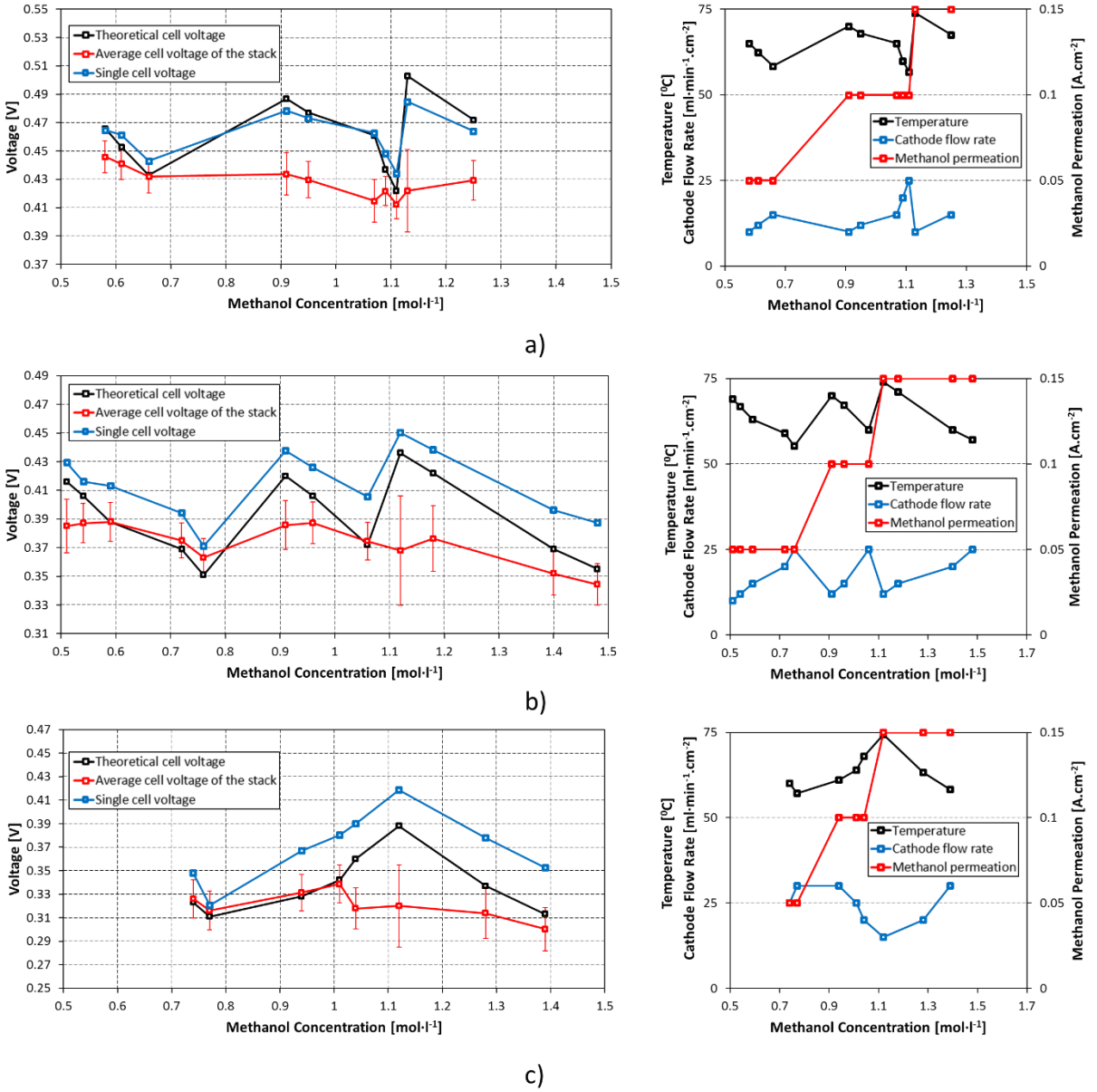

Figure 7. Comparison of the voltage values between the theoretical model, single cell testing and average cell of the short stack testing at (a) 0.10 A·cm^{-2}, (b) 0.15 A·cm^{-2} and (c) 0.20 A·cm^{-2} for various methanol concentrations and the relationships between the methanol concentrations and cell temperature, methanol permeation and the cathode flow rate (right-hand graphs).

Comparison of the results shows good agreement between the numerical calculations and single cell test voltage at all operating conditions. The shapes of the curves are identical, and the difference in absolute values is ± 0.01 V for a current density of 0.1 A·cm^{-2}. For higher current densities the actual voltage of the single cells is higher than the theoretical cell voltage. The difference is 0.01 to 0.02 V for a current density of 0.15 A·cm^{-2} and 0.02 to 0.03 V for a current density of 0.2 A·cm^{-2}. The cell voltage of the short stack shows relatively good agreement for some operating conditions and higher deviations at other operating conditions. The reason for this is not evident from figure 7, but becomes clear form figure 8 and will be discussed there.

The results show that 0.465 V is achieved from a single cell test and theoretical model at 0.10 A·cm^{-2}, 65 °C and 0.55 M, which is higher than the short stack results. On the other hand, the highest individual cell voltage in the stack is found to be 0.465 V in the second cell of the stack under these conditions. Voltage outputs decrease with lower temperatures and higher CFR for concentrations lower than 0.7 M when methanol crossover current density remains constant. Although similar voltages can be achieved from single cell tests and theoretical models at 0.10 A·cm^{-2} and 0.15 A·cm^{-2} methanol crossover current densities, lower voltage values are obtained from the short stack. For instance, at 1.25 M concentration, 65 °C temperature, 15 ml·cm^{-2}·min^{-1} CFR and 0.15 A·cm^{-2} methanol permeation yield 0.472 V from the

theoretical model, 0.465 V from the single cell test and 0.445 V, 0.44 V, 0.43 V, 0.42 V and 0.41 V from the short stack test results for the third, second, fourth, fifth and first cells, respectively (see Figure 7a). This indicates that thermal losses from the stack are responsible for part of the difference, because the first and fifth cells have the lowest cell voltage. However, the second to fourth cell also do not reach the same voltage of the single cell, so there must be another reason as well.

The effect of concentration on the voltage can be also observed in Fig 7. The single cell, average cell and theoretical cell voltage of DMFC stack increases when the methanol concentration increases from 0.8 mol·l-1 to 1.1 mol·l-1 at the current density of 0.20 A·cm-2. This voltage increment is found to be up to 0.08 V. For this methanol concentration range (0.8-1.1 mol·l-1), the results are compatible with the results of Schulze Lohoff et al. [18] and Dohle et al. [36].

In Figure 8 the same data as in the left graph of Figure 7b are plotted as a function of temperature. For a 0.15 A·cm^{-2} current density, the voltage obtained from the single cell test is higher than from short stack tests for all methanol concentrations except 0.75 M. This exception is caused by the highest CFR and the lowest operating temperature condition. Almost the same difference between the single cell test and theoretical model (about 0.02 V) results are observed for all data points. Although the voltages obtained from the single cell test are higher than those obtained from the short stack tests, the theoretical model results show similarity with the average cell voltage obtained from short stack testing at relatively lower temperatures (50-60 °C). Higher differences occurred at lower CFR (10-15 ml·cm^{-2}·min^{-1}) and higher operating temperature (65-75 °C) for 1.12 M methanol concentrations and 0.150 A·cm^{-2} methanol crossover current density, as shown in Figure 8. At the same time the standard deviation between the individual cell voltages of the short stack, as indicated by error bars in Figure 8, increases. Since the higher cell temperatures are obtained at low cathodic flow rates and high methanol crossover rates it is clear that air is fed into the cells only at very small excess. Thus small deviations in air flow among the different cells will have a big influence. This is presumably the reason for the deviation among cell voltages and subsequently reduced stack performance. Under those conditions, a higher air flow rate will not have a big effect on cell voltage, while a lower air flow rate will lead to a significantly reduced cell voltage.

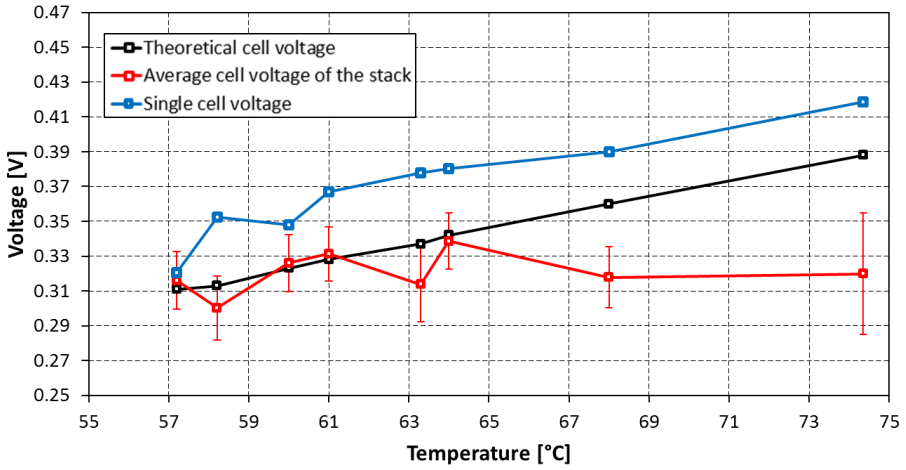

Figure 8. Comparison of the voltage values between the theoretical model, single cell testing and average cell of the short stack testing 0.15 A·cm^{-2} as a function of the cell temperature using the same data as in Figure 7b.

For a 0.20 A·cm^{-2} current density, the third cell gives the highest voltage outputs for all methanol concentrations. The voltage results of the theoretical model are quite similar, with the average cell voltage of the short stack at a current density of 0.10 A·cm^{-2}. The single cell test results show good agreement with the model and stack results at lower concentrations (0.7-0.9 M) for 0.20 A·cm^{-2} current density (Figure 7c). Generally, it can be observed that in a stack there is always a small difference between the individual cell voltages. While it can be assumed that the cells at the endplates are a little bit cooler, the differences amongst the internal cells can be caused by small differences in catalyst loading, the anode flow rate or the cathode flow rate. These can easily be caused by small geometric differences in the cell inlet and outlet regions. The increase of the standard deviation at low CFR indicates that uneven distribution of the air among the five cells might be the main reason for this and for the reduced average cell voltage here.

In Figure 8, it is also seen that the voltage increases with increasing DMFC temperature. For example, when the temperature increases 10 ˚C, the increment of theoretical cell voltage is found as 0.06 V. This result shows very good agreement with results of 3-D multi-phase numerical model of Sun et al. [37] when the current density is 0.15 A·cm-2.

While the simulation allows for the exclusion of effects such as impurities or heat losses, it is limited by assumptions that are necessary in order to keep the model simple. The operating conditions in single cells can still be controlled very precisely, while the effects of different catalysts, catalyst layer structures, the blocking of pores by water and similar effects can be analyzed. One must be careful, however, to choose realistic operating conditions. A self-heating stack is always operated at realistic operating conditions and effects like mass flow distribution amongst the cells can be studied. The effort, however, is highest and effects like heat loss over the stack surfaces are greater for short stacks or stacks with smaller cells.

4. Conclusions

In the present study, three methods (single cell testing, short-stack testing and mathematical 1D model) for the DMFC characterization are presented. This paper mainly aims to obtain in-depth knowledge of effect of the operating parameters on the DMFC performance. In addition, strengths and weaknesses of these methods are given. Therefore, DMFC voltage outputs from a single cell and short stack were compared to the results from a 1D mathematical model. The effects of the operating temperatures, CFR, methanol permeation and methanol concentration on the voltage outputs are investigated for various current density values. The main conclusions derived are as follows:

- The results show very good agreement at lower methanol crossover rates and therefore lower temperatures.
- It is found that when the operating temperature is 57 °C, a good match is observed between three methods.
- Voltage outputs drop with increasing CFR and decreasing temperatures for all methanol concentrations and current densities. This voltage drop is higher for the theoretical model than for the real cells.
- The differences between the model and single cell test results are small, but it increase with higher current density.
- The voltage differences between the cells of the short stack increase with higher current density and methanol concentration. Under these conditions, the stack temperatures are very high, and so thermal losses over the endplates can lead to lower temperatures in the adjacent cells.
- High methanol permeation causes a higher voltage drop in cells of the short stack, and so the average cell voltage of the short stack is lower. This could also be due to a loss of heat in the short stack.

The comparisons between the voltage results under different operating conditions with modeling and testing methods show that the voltage values of a 1D model and single cell tests can be used accurately enough for the calculation of the voltage outputs for a DMFC stack, which is easier to obtain compared to stack testing. It is important to understand the scope and limitation of each testing method in order to obtain the best possible results without excessive effort.

REFERENCES

[1] Larminie J., Dicks A. (2003). Fuel cell system explained. 2nd Ed., Wiley Press. ISBN: 0-470-84857-X. 2003.

[2] Goor, M., Menkin, S., & Peled, E. (2019). High power direct methanol fuel cell for mobility and portable applications. International Journal of Hydrogen Energy, 44(5), 3138-3143.

[3] Ercelik, M., Ozden, A., Seker, E., & Colpan, C. O. (2017). Characterization and performance evaluation of PtRu/CTiO2 anode electrocatalyst for DMFC applications. International Journal of Hydrogen Energy, 42(33), 21518-21529.

[4] Li X., Faghri A. (2013). Review and advances of direct methanol fuel cells (DMFCs) part I: Design, fabrication, and testing with high concentration methanol solutions. International Journal of Power Sources, 226, 233–240.

[5] Karaoğlan, M. U., İnce, A. C., Colpan, C. O., Glüsen, A., Kuralay, N. S., Müller, M., & Stolten, D. (2019). Simulation of a hybrid vehicle powertrain having direct methanol fuel cell system through a semi-theoretical approach. International Journal of Hydrogen Energy, 44(34), 18981-18992.

[6] Colpan C.O., Cruickshank C.A., Matida E., Hamdullahpur F. (2011). 1D - modeling of a flowing electrolyte-direct methanol fuel cell. International Journal of Power Sources, 196, 3572–3582.

[7] Ozden, A., Ercelik, M., Ozdemir, Y., Devrim, Y., & Colpan, C. O. (2017). Enhancement of direct methanol fuel cell performance through the inclusion of zirconium phosphate. International Journal of Hydrogen Energy, 42(33), 21501-21517.

[8] Ozden, A., Ercelik, M., Devrim, Y., Colpan, C. O., & Hamdullahpur, F. (2017). Evaluation of sulfonated polysulfone/zirconium hydrogen phosphate composite membranes for direct methanol fuel cells. Electrochimica Acta, 256, 196-210.

[9] Wang, S., Jing, S., Mao, Z., & Xie, X. (2016). Polarization distribution and theoretical fitting of direct methanol fuel cell. International Journal of Hydrogen Energy, 41(36), 16247-16253.

[10] Jung D.H., Lee C.H., Kim C.S., Shin D.R. (1998). Performance of a direct methanol polymer electrolyte fuel cell. International Journal of Power Sources, 71, 169–173.

[11] Ge J., Liu H. (2005). Experimental studies of a direct methanol fuel cell. International Journal of Power Sources, 142, 56–69.

[12] Thomas, S. C., Ren, X., Gottesfeld, S., & Zelenay, P. (2002). Direct methanol fuel cells: progress in cell performance and cathode research. Electrochimica Acta, 47(22-23), 3741-3748.

[13] Dohle H., Wippermann K. (2004). Experimental evaluation and semi-empirical modeling of *U/I* characteristics and methanol permeation of a direct methanol fuel cell. International Journal of Power Sources, 135, 152–164.

[14] Chen C.Y., Shiu J.Y., Lee Y.S. (2006). Development of a small DMFC bipolar plate stack for portable applications. International Journal of Power Sources, 159, 1042–1047.

[15] Manokaran A., Vijayakumar R., Thomman T.N., Sridhar P., Pitchumani S., Shukla A.K. (2011). A self-supported 40W direct methanol fuel cell system. Journal of Chemical Sciences, 123, 343–347.

[16] Kim D., Lee J., Lim T.H, Oh I.H., Ha H.Y. (2006). Operational characteristics of a 50W DMFC stack. International Journal of Power Sources, 155, 203–212.

[17] Joh H.I., Hwang S.Y., Cho J.H., Ha T.J., Kim S.K., Moon S.H., Ha H.Y. (2008). Development and characteristics of a 400 W-class direct methanol fuel cell stack. International Journal of Hydrogen Energy, 33, 7153–7162.

[18] Schulze Lohoff, A., Kimiaie, N., & Blum, L. (2016). The application of design of experiments and response surface methodology to the characterization of a direct methanol fuel cell stack. International Journal of Hydrogen Energy, 41(28), 12222-12230.

[19] Dohle H., Schmitz H., Bewer T., Mergel J., Stolten D. (2002). Development of a compact 500 W class direct methanol fuel cell stack. International Journal of Power Sources, 106, 313–322.

[20] Garcia B., Sethuraman V.A., Weidner J.W., White R.E., Dougal R. (2004). Mathematical Model of a Direct Methanol Fuel Cell. International Journal of Fuel Cell Science and Technology, 1, 43–48.

[21] Oliveira V.B., Falcao D.S., Rangel C.M., Pinto A.M.F.R. (2007). A comparative study of approaches to direct methanol fuel cells modelling. International Journal of Hydrogen Energy, 32, 415–424.

[22] Lee J., Lee S., Han D., Gwaak G., Ju H. (2017). Numerical modeling and simulations of active direct methanol fuel cell (DMFC) systems under various ambient temperatures and operating conditions. International Journal of Hydrogen Energy, 42, 1736–1750.

[23] Colpan C.O., Fung A., Hamdullahpur F. (2012). 2D modeling of a flowing-electrolyte direct methanol fuel cell. International Journal of Power Sources, 209, 301–311.

[24] Kjeang E., Goldak J., Golriz M.R., Gu J., James D., Kordesch K. (2006). A parametric study of methanol crossover in a flowing electrolyte-direct methanol fuel cell. International Journal of Power Sources, 153, 89–99.

[25] Ge J., Liu H. (2006). A three-dimensional mathematical model for liquid-fed direct methanol fuel cells. International Journal of Power Sources, 160, 413–421.

[26] Colpan, C.O., & Ouellette, D. (2018). Three dimensional modeling of a FE-DMFC short-stack. International Journal of Hydrogen Energy, 43(11), 5951-5960.

[27] Casalegno A., Marchesi R. (2008). DMFC anode polarization: Experimental analysis and model validation. International Journal of Power Sources, 175, 372–382.

[28] Casalegno A., Marchesi R. (2008). DMFC performance and methanol cross-over: Experimental analysis and model validation. International Journal of Power Sources, 185, 318–330.

[29] Falcao D.S., Oliveira V.B., Rangel C.M., Pinto A.M.F.R. (2015). Experimental and modeling studies of a micro direct methanol fuel cell. Renewable Energy, 74, 464–470.

[30] Müller, M., Kimiaie, N., Glüsen, A., (2014). Direct methanol fuel cell systems for backup power – Influence of the standby procedure on the lifetime. International Journal of Hydrogen Energy, 39, 21739-21745.

[31] Knights, S.D., Colbow, K.M., St-Pierre, J., Wilkinson, D.P., (2004). Aging mechanisms and lifetime of PEFC and DMFC. International Journal of Power Sources, 127, 127-134.

[32] Ince, A.C., Karaoglan, M.U., Glüsen, A., Colpan, C.O., Müller, M., Stolten, D. (2019). Semiempirical thermodynamic modeling of a direct methanol fuel cell system. International Journal of Energy Research, 43, 3601-3615.

[33] Xu, Q., Zhang, W., Zhao, J., Xing, L., Ma, Q., Xu, L., & Su, H. (2018). Effect of air supply on the performance of an active direct methanol fuel cell (DMFC) fed with neat methanol. International Journal of Green Energy, 15(3), 181-188.

[34] Kumar, P., Dutta, K., & Kundu, P. P. (2014). Enhanced performance of direct methanol fuel cells: a study on the combined effect of various supporting electrolytes, flow channel designs and operating temperatures. International Journal of Energy Research, 38(1), 41-50.

[35] Colpan, C. O., Ouellette, D., Glüsen, A., Müller, M., & Stolten, D. (2017). Reduction of methanol crossover in a flowing electrolyte-direct methanol fuel cell. International Journal of Hydrogen Energy, 42(33), 21530-21545.

[36] Dohle, H., Divisek, J., & Jung, R. (2000). Process engineering of the direct methanol fuel cell. Journal of Power Sources, 86(1-2), 469-477.

[37] Sun, J., Zhang, G., Guo, T., Jiao, K., & Huang, X. (2018). A three-dimensional multi-phase numerical model of DMFC utilizing Eulerian-Eulerian model. Applied Thermal Engineering, 132, 140-153.